



## **Journal of Geophysical Research: Oceans**

## **RESEARCH ARTICLE**

10.1002/2014JC009946

#### **Kev Points:**

- Direct measurements show 4.6 Sv of inflow across the IFR toward the Nordic Seas
- Flows across the IFR and through the FSC are have high short-term variability

#### **Supporting Information:**

- Readme
- Figure S1
- Figure S2
- Figure S3 • Figure S4
- Figure S5
- Figure S6 • Figure S7

#### **Correspondence to:**

K. H. Childers, katelin.childers@stonybrook.edu

#### Citation:

Childers, K. H., C. N. Flagg, and T. Rossby (2014), Direct velocity observations of volume flux between Iceland and the Shetland Islands, J. Geophys. Res. Oceans, 119, 5934-5944, doi:10.1002/2014JC009946.

Received 9 MAR 2014 Accepted 15 AUG 2014 Accepted article online 25 AUG 2014 Published online 11 SEP 2014

## Direct velocity observations of volume flux between Iceland and the Shetland Islands

Katelin H. Childers<sup>1</sup>, Charles N. Flagg<sup>1</sup>, and Thomas Rossby<sup>2</sup>

<sup>1</sup>School of Marine and Atmospheric Science, Stony Brook University, Stony Brook, New York, USA, <sup>2</sup>Graduate School of Oceanography, University of Rhode Island, Kingston, Rhode Island, USA

Abstract Atlantic Waters flowing northward into the Nordic Seas are important for their role as an early indicator of changes to deepwater formation. As such, this requires a fundamental understanding of the pathways and volume fluxes through the primary passageways from the Atlantic into the Nordic Seas. A mean annual volume transport of 6.1  $\pm$  0.3 Sv was observed flowing in above the  $\sigma_t$  = 27.8 isopycnal (a proxy for the lower limit of Atlantic Water depth), through the Faroe Shetland Channel (FSC) and over the Iceland Faroes Ridge (IFR) from March 2008 to June 2012, using repeat velocity sections obtained from a vessel mounted Acoustic Doppler Current Profiler (ADCP). A new vessel route has expanded the spatial coverage of FSC observations and reveals a difference in average inflow transport, which most likely results from an interannual variation in the total transport through the FSC, which in turn is tied to a weakening of the southerly flow over the western slope of the channel. This interannual variability has increased the mean transport through the FSC from 0.9 Sv observed over the first 2 years of this program by Rossby and Flagg (2012) to a 4.5 year mean of 1.7  $\pm$  0.2 Sv, which emphasizes the importance of knowing the flow along the Faroese shelf. Interannual fluctuations in transport observed over the IFR are related to the width of the inflow over the Faroese half of the ridge.

## 1. Introduction

The primary Atlantic Water inflows to the Arctic Mediterranean occur through the Faroe Shetland Channel (FSC) and over the Iceland Faroes Ridge (IFR). These waters enter the northern North Atlantic as part of the North Atlantic Current and ultimately source the dense water production in the Nordic Seas. A description of the mean current structure and northward flux through the Shetland-Faroe-Iceland opening toward the Norwegian Sea has been developed using nearly 4.5 years of observational velocity data collected by the M/F Norröna. This report expands upon the first summary paper [Rossby and Flagg, 2012; hereafter RF] including data from the two most recent years (2011 and 2012), as well as a comparison with transports across the two FSC routes now in use by the ship (Figure 1).

The earliest depiction of currents and eddies between Iceland, the Faroes, and Norway is the 1539 Carta Marina map of Olanus Magnus in the sixteenth century. Three centuries later, marine research gained momentum with the hydrographic and circulation observations by Helland-Hansen and Nansen in the late nineteenth and early twentieth centuries [Helland-Hansen and Nansen, 1909]. Regular observations of potential temperature and salinity have been collected since the 1970s [Coachman and Aagaard, 1974], and recent descriptions of the transport through the FSC and IFR rely heavily on moored Acoustic Doppler Current Profilers (ADCPs) and hydrographic data along the Fair Isle Munken (FIM) line, south of the Norröna's Southern track and line N, north of the Faroes [Hansen et al., 2003; Hughes et al., 2006; Sherwin et al., 2008; Hansen et al., 2010]. The Faroes Fisheries Lab and Fisheries Research Services, Abderdeen have monitored standard hydrographic locations along the FIM line since 1994 [Sherwin et al., 2008], which are supplemented by ADCP deployments originally as part of the Nordic-WOCE project and later incorporated into the VEINs and MAIA projects [Hughes et al., 2006]. For almost 20 years, five to seven moored, upward looking ADCPs have been in use along the line from the 300 m isobath on the western Faroese slope to the Shetland Shelf [Hughes et al., 2006]. The westernmost ADCP was removed a few years into the study due to the low transport observed at that particular location [Hughes et al., 2006]. Most of the published results from this section use the location of this ADCP as the western point of transport integration, resulting in a lack of direct observations of the southerly flow on the Faroese side, and report FSC transports of 2.7 Sv [Berx et al., 2013], 3.5 Sv [Sherwin et al., 2008], and 3.9 Sv [Hughes

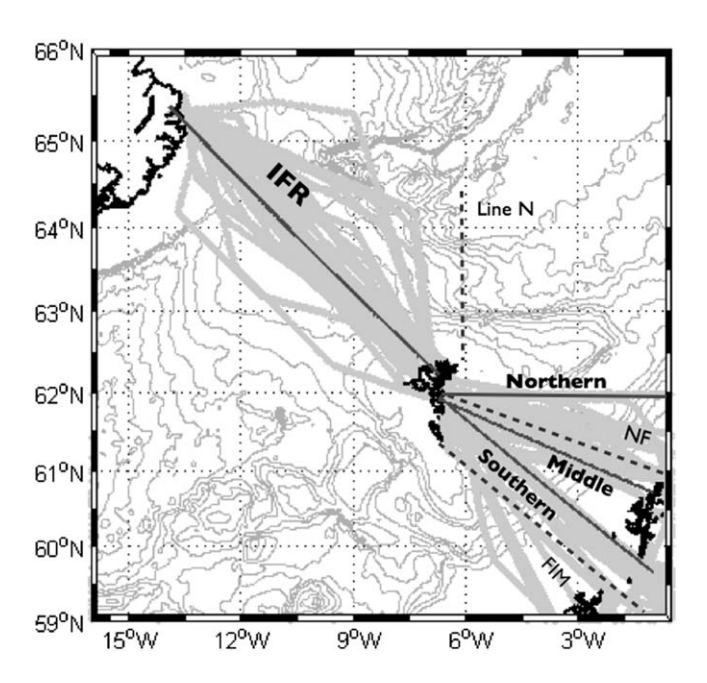


Figure 1. Map of Norröna crossings (gray dots) and mean locations of each transect (dark gray lines). Dotted lines are the Nolsa Flugga (NF) line, Fair Isle Munken (FIM) line, and line N. Bathymetry contours are from 250 to 3000 m in increments of 250 m.

et al., 2006]. Similar methods along line N show inflow of Atlantic Water (AW) across the IFR to be 3.5  $\pm$  0.5 Sv [Hansen et al., 2003, 2010].

The Norröna velocity data approach the estimation of transport from a different perspective. The use of vessel mounted, rather than moored ADCP data, significantly improves the horizontal resolution and increases coverage in the shallow regions of the FSC. Direct observations of velocity across both sections also eliminate any dependence on geostrophic estimates between stations. In particular, a more robust image emerges for the IFR transport by sampling across the entire section and removing the need to account for other incoming eastward flows along the Iceland Faroes Front, which cross line N along with the AW inflows [Hansen et al., 2003, 2010].

Waters moving from the Atlantic toward the Nordic Seas flow over the eastern (right in this figures) halves of both the FSC and IFR sections as the wedge shaped Shetland Slope Current (SSC) in the FSC and a less structured flow over the IFR (Figures 4, 5, and 8) [RF; Berx et al., 2013; Hughes et al., 2006; Sherwin et al., 2008]. Adopting the terminology of Hansen et al. [2003], we will refer to currents crossing the Iceland-Faroes-Scotland Ridge from the Atlantic toward the Nordic Seas and Arctic Ocean as "inflows" and waters going from the Nordic Seas toward the Atlantic as "outflows." In RF, 5.9 Sv of inflow was measured over the full depth of the southeastern half of the IFR and -1.5 Sv of outflow over the northwest. Through the FSC, 4.1 Sv of inflow was reported and -3.2 Sv of surface outflow entered the north Atlantic above the  $\sigma_{\rm t}=27.8$ isopycnal. Of particular note in RF, is the presence of the stronger than anticipated southward outflow through the western FSC, reducing the total mean inflow through the channel. The authors postulated roughly half of this flow to be the result of tidally rectified AW entering over the IFR and circling anticyclonically around the Faroes into the FSC. They further hypothesized that the other half of the southward flow may join the northeasterly Shetland Slope Current as evidenced by the width of the northward velocities extending farther west than the high salinity wedge [RF]. Subsequent data collection by the Norröna along a second route across the FSC allows us to explore questions about temporal and spatial variability, a major objective of this study.

Short-term variability in this region makes capturing a true "mean" image difficult and subject to velocity changes over a variety of timescales. An active eddy field, strong tidal oscillations, and interactions with steep and irregular topography impose further challenges. The results presented here show that even one additional year of data (compared to RF) can have an impact on the overall description of velocity and transport in this region. A complete picture may only be possible after data have been collected over a full cycle of the AMO [Häkkinen et al., 2013] or NAO [Sherwin et al., 2008], which has been shown to influence the strength of the gyres and currents in the Nordic Seas and Iceland Basin [Jakobsen et al., 2003] and the development of persistent eddies in the FSC, in turn adjusting the mean path of the SSC [Chafik, 2012]. In addition, drifter analyses by Valdimarsson and Malmberg [1999] found drifter behavior between Iceland and the Faroes to alter in conjunction with the phase of the NAO, which has been in a low phase for the majority (2009–2012) of data collection by the Norröna. However, the relatively consistent pattern of flow over the IFR and good agreement between coincident periods across the two FSC routes, as well as the observations by Jakobsen et al. [2003] that the changing circulation strengths north and south of the Iceland-Faroes-

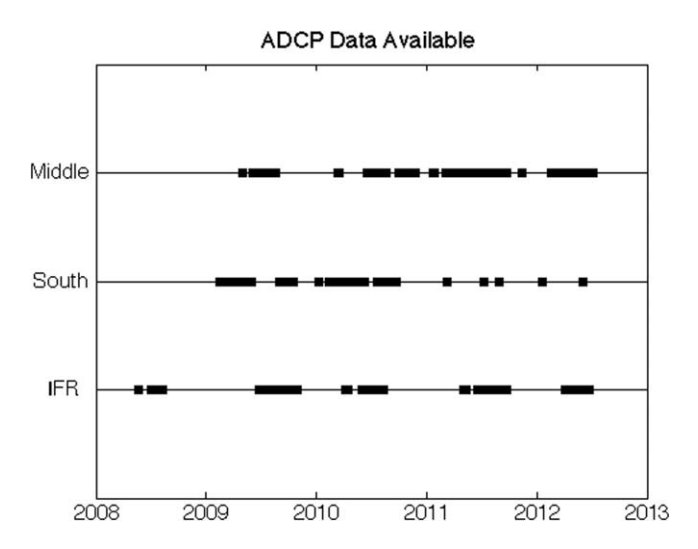


Figure 2. Date of data collection along each track.

Scotland Ridge may not exert significant influence on the magnitude of transport across the IFR, suggest that the velocities and transports presented here are a good approximation of the average long-term surface inflows from the Atlantic to the Nordic Seas. This paper will first summarize the mean velocities and transports through the FSC and IFR then consider the temporal and structural variability in relation to previous studies of the region.

#### 2. Data and Methods

The data set is built up of direct velocity observations from a vessel mounted 75 kHz RDI Ocean Surveyor

ADCP run in narrow-band mode to reach depths of up to 600 m. Vessel heading is provided by a Thales ADU-5 once per second, which in addition to errors in the single ping accuracy from the ADCP result in a total uncertainty of 0.025 m/s [RF]. The Norröna travels weekly from Denmark to Iceland and back along four primary routes: (1) from Seydisfjördur, Iceland to Tórshavn along the Iceland Faroes Ridge; (2) from Tórshavn to Bergen, hereafter referred to as the "Northern track"; (3) from Tórshavn to Hirtshals, Denmark via a route north of the Shetland Islands, the "Middle track"; and (4) from Torshavn to Hirtshals, Hantsholm or Esbjerg, Denmark via a route south of the Shetland Islands, the "Southern track" (Figure 1). An expedited schedule during the summer shortens the round trip travel time and provides the opportunity for more than 50 round trip crossings per transect each year. Over the course of this study, the Northern route has been abandoned. Bubbles underneath the vessel prevent data collection in conditions of high sea swell due to the heaving of the bow and breaching of the large bow-thruster openings. These scoop large volumes of air that are subducted and entrained into the flow along the hull, disrupting data collection during the winter and spring. Following the final adjustments during a January 2009 dry docking, the data return over the IFR doubled from full coverage during six transect crossings in 2008 to 12 in 2009 (Figure 2). This level of data return has continued, with 10–

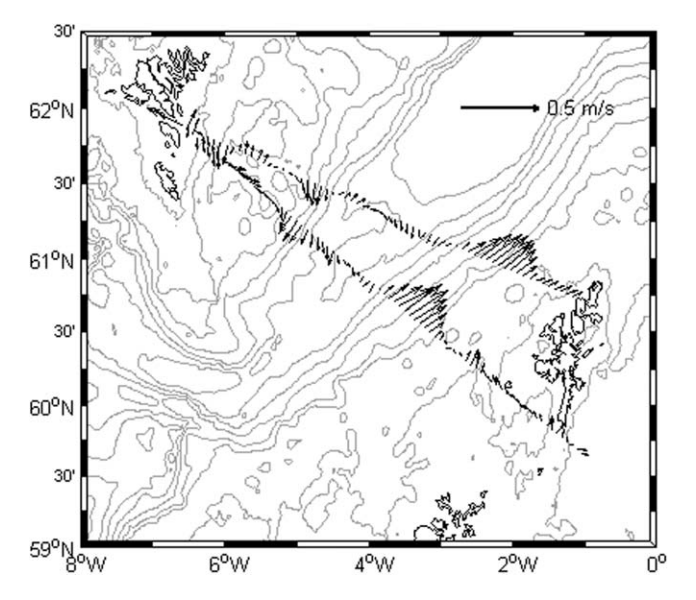


**Figure 3.** Map of surface FSC surface velocities (mean of upper 200 m) and local topography from 100 to 1300 m in increments of 200 m.

14 successful observations of the IFR section per year and more than 20 observations per year through the FSC. Presently, the ADCP sits about 1/3 of the way back from the bow in a streamlined fairing that extends 0.2 m below the hull. Individual pings along each section are first averaged into 3 min ensembles, and then collapsed onto a mean line for each track (Figure 1). The data are then further averaged into bins of 5 km in the horizontal and 20 m vertically.

Several water masses move through the FSC and over the IFR, making an accurate estimate of the local temperature and salinity structure important in determining the volume of AW entering the Nordic Seas. To help define the water masses, hydrographic data are taken from the ICES

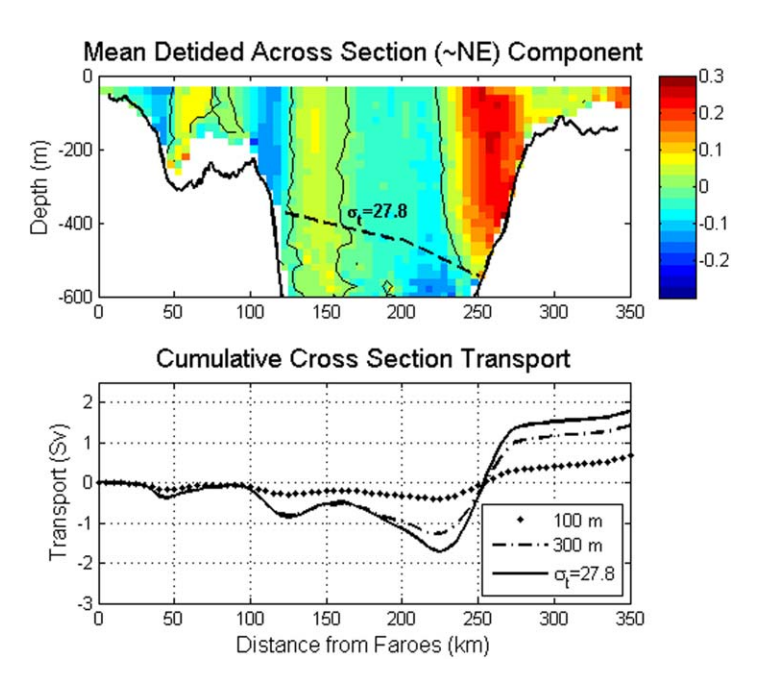


**Figure 4.** Mean  $\sim$ NE velocities normal to (top) the FSC Middle track and (bottom) cumulative across track transport. The black solid line includes all available data over the full AW depth from March 2008 to June 2012, a total of 88 sections.

database using the online data portal. All available temperature and salinity measurements collected from March 2008 to June 2012 and within 50 km of each transect were used to construct mean temperature, salinity, and density profiles for each section (supporting information Figures S2-S5). In the FSC, most hydrographic data come from regular monitoring of the FIM and Nolso Flugga lines just south and north of the Norröna transects. Each three month season (DJF, MAM, JJA, SON) has at least 50 available stations except for DJF 2011, which has 44. Similar to the ADCP data, the hydrography is also slightly biased toward the summer and fall, when a greater number of sections are available. Hydrography over the IFR is more limited both spatially

and temporally. Supporting information Figure S2 shows the location of available temperature and salinity profiles, which are largely concentrated near the Faroe shelf and slope.

Here we refer to waters with potential densities less than  $\sigma_t$  = 27.8 as AW, which is consistent with previous studies by von Appen et al. [2014], Våge et al. [2013], and RF. Complementary AW definitions in recent analyses of the region using the average depths of the 35.05 PSU isohaline [Hansen et al., 2010] and 5°C isotherm [Berx et al., 2013], fall within 60 m of the isopycnal determination across both FSC sections (supporting information Figures S3 and S4). Significant changes in seasonal stratification exist in this region [Larsen et al., 2008; Borenäs et al., 2001; Gaard and Hansen, 2000], however, observations of the depth of the  $\sigma_t$  = 27.8 isopycnal for each FSC transect vary seasonally by less than 100 m. Without concurrent hydrographic sections available during each transect crossing, we use the mean isopycnal depth over the nearly 4.5 year collection period as an indicator of the vertical extent of AW. This assumption introduces an estimated error of 0.02 Sv for the Southern route and 0.01 Sv for the Middle route, associated with a 100 m vertical difference in the lower limit of transport integration.

The methods of ADCP data collection utilized in this analysis are not conducive to traditional procedures of tidal characterization due to the lack of simultaneous observations or temporally frequent data at any given location. A method using least squares fitting to a distribution of interpolation knots [*Dunn*, 2002; *Wang et al.*, 2004] is used to separate and characterize the tides appearing in the observations. With this method, the spatial dependence of the tidal velocity components in the upper 100 m of the water column is represented by Gaussian basis functions permitting estimation of the tides at the irregularly spaced observation locations [*Wang et al.*, 2004]. The resulting tidal amplitudes and phases compare favorably to a numerical model produced by the Earth and Space Research (ESR) Institute in collaboration with Oregon State University [*Egbert and Erofeeva*, 2002], and to published tidal ellipses from moored ADCP data on the Faroes shelf [*Larsen et al.*, 2000].

The detided, bin-averaged velocity data set forms the basis for all subsequent analyses including the computation of the across track volume flux or transport in Sverdrups (1 Sv =  $10^6$  m<sup>3</sup>/s) through each bin as

$$Q = A_{bin} \times u_{bin} \tag{1}$$

where  $A_{bin}$  is the area of each bin and  $u_{bin}$  is the velocity normal to it. All available data falling within each geographical bin are used to compute the mean along and across track velocity for that particular bin. This method results in some bins having a greater number of samples when spatial coverage over a transect is incomplete. The total transports for each section are obtained by summing the bin transports along each transect over the

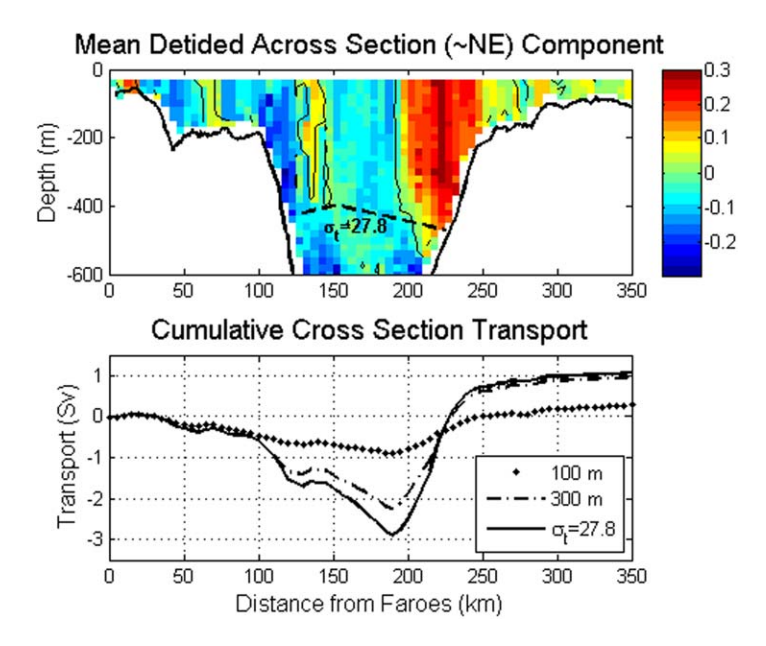


**Figure 5.** Mean ~NE velocities normal to (top) the FSC Southern track and (bottom) cumulative across track transport. The black solid line includes all available data over the full AW depth from March 2008 to June 2012, a total of 44 sections.

depths associated with inflowing Atlantic Water (above the  $\sigma_t = 27.8$  isopycnal, Figures 4 and 5). Velocity uncertainties were calculated using the observed standard deviation in across section velocity to determine the total single section uncertainty for each transect crossing. Velocity and transport uncertainties are the standard error of the mean, with the degrees of freedom equal to the number of transect crossings, assuming that the individual crossings separated by 1-4 days represent independent observations.

Steep and variable bathymetry, such as in this region, influence mesoscale flows by guiding them along isobaths and inducing nonlinear interactions. For

the consideration of along topography flow, we use bathymetry for the region from NASA's ETOPO2 topographical data set [*U.S. Department of Commerce et al.*, 2006]. The resolution is 2 min of both latitude and longitude (approximately 4 and 2 km, respectively, over the domain under study) and 1 m in the vertical [*U.S. Department of Commerce et al.*, 2006]. A range of frequently sampled velocity bins were selected for comparison to the direction of nearby f/H contours, computed using the ETOPO2 bathymetry. Although not without temporal gaps, the time series of velocity vector orientation at nearby locations serves as an indicator for topographic steering strength.

## 3. Results

Results from the FSC will be discussed first, followed by the IFR. The FSC analysis will be broken into an examination of the Shetland Slope Current structure and variability, followed by a consideration of the southward flow on the Faroese slope.

#### 3.1. Flow Through the Faroe Shetland Channel

Inflow through the FSC is dominated by the Shetland Slope Current flowing along the steepest portion of the Scottish slope, and a southward outflow along the Faroese slope (Figure 3). In late 2010, a shift in data collection occurred from more frequent use of the Southern route to a favored use of the Middle route. From 2008 to 2012, 132 crossings (88 via the Middle route and 44 using the Southern) have contributed to the overall coverage of the FSC, and in general the velocity structure is similar for both routes. The best data returns occur near the surface, with the number of samples dropping roughly in half below 500 m and halved again below 600 m for both tracks. Standard errors in the channel range from 1 to 5.7 cm/s per bin, and integrated transect uncertainties of the surface inflow ( $\sigma_{\rm t}$  < 27.8) are 0.2 Sv for both the Middle and Southern routes.

The mean inflow through the FSC east of 200 km from the Faroes and above the  $\sigma_{\rm t}=27.8$  isopycnal is  $3.4\pm0.2$  Sv (Middle section) and  $4.0\pm0.23$  Sv (Southern section) primarily attributable to the Shetland Slope Current. The Slope Current dominates the eastern shelf region along both transects with the Middle track showing a slightly weaker core (Figures 4 and 5). Interannual variations in the Shetland Slope Current transport across both FSC sections range from 3.1 Sv at its weakest in 2009 to 3.7 Sv at its strongest in 2011. The vertical structure of the upper water column of both FSC routes is largely depth independent, resulting in gradual increases of cross-transect transport with integration depth (Figures 4 and 5).

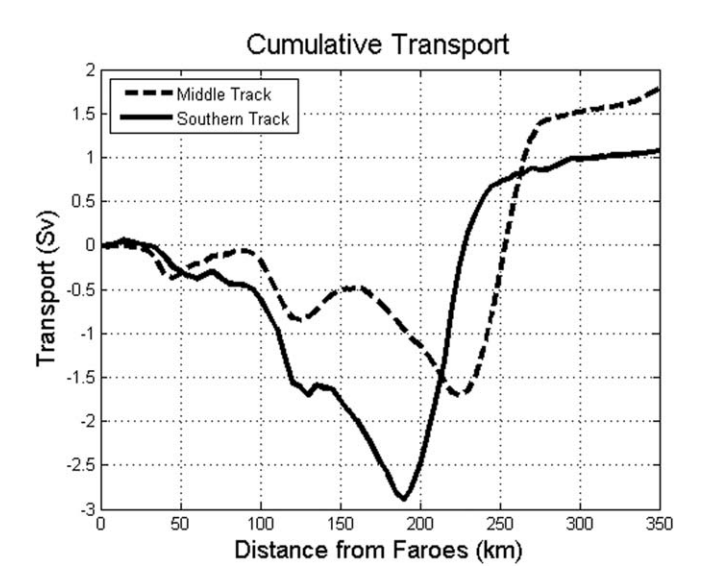
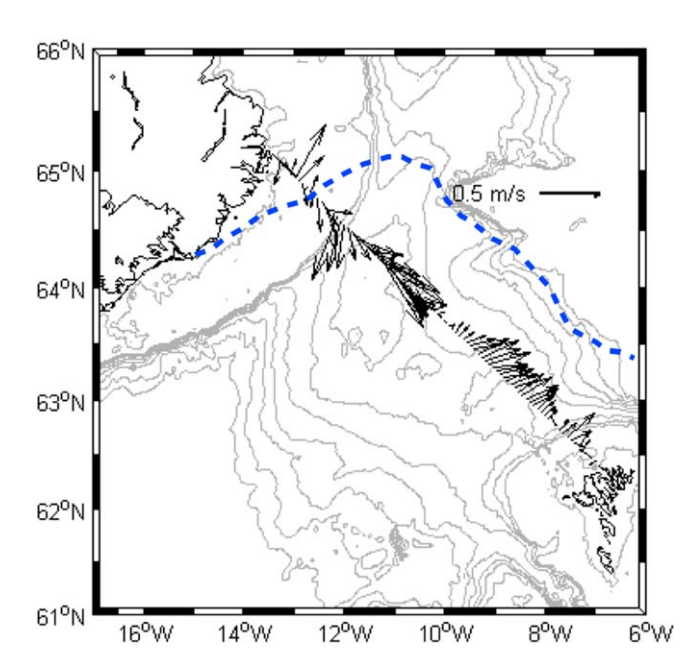


Figure 6. Cumulative transport for each track with distance along the FSC.

The switch from the Southern route to the Middle transect introduced a puzzling discrepancy in transport estimates (Figure 6). The Norröna sampled the Southern section heavily from March 2008 to August 2010 (87% of the total Southern transects) and the Middle track from June 2010 to June 2012 (71% of the total Middle transects). Despite a closed channel between the two sections, the observed magnitude of the average northeast transport was higher through the Middle route. However, when considering only a few early sections from the Middle track nearly contemporaneous with those from the Southern track, the mean transport estimate agrees to within 0.8 Sv. Only after the inclusion of the last

year and a half of data does the total transport increase by almost a full Sv to 1.7 Sv through the Middle track, suggesting a temporal change in flow through the channel as the source for the transect differences. During periods of roughly coincident coverage, such as during the summer of 2010 as well as isolated crossings in 2009, 2011, and 2012 (Figure 2), when the ship sampled along both routes over a short time span (less than 2 weeks), the structure and surface transport agrees well across both sections, despite the influence of local eddy activity in the channel. Given the similarity of the crossings of each track across the FSC, it is reasonable to combine the full set of FSC observations for the analysis of interannual fluctuations.

The combined time series for the FSC has a reduced standard error (0.19 Sv) and an improved temporal and spatial coverage of the surface outflow on the Faroese shelf and slope. Opposite the Shetland Slope Current, a  $\sim$ 30 km band of southerly flow along the Faroese slope comprises most of the surface outflows, accounting for -1.0 Sv, on average, toward the Atlantic above the  $\sigma_{\rm t}=27.8$  isopycnal (Table 1). The largely



**Figure 7.** Map of surface IFR surface velocities (mean of upper 200 m) and local topography from 100 to 1500 m in increments of 200 m. The blue dotted line indicates the mean position of the Iceland Faroes Front.

depth-independent outflow shows an interannual variability of up to half of its average magnitude. It peaks from 2008 to 2010, weakens considerably in 2011, and partially rebounds in 2012. Temperature and salinity profiles show a clear distinction between the warmer and saltier inflow waters of the SSC and the relatively cooler and fresher surface outflows over the Faroese shelf and slope (supporting information Figures S3 and S4). The high salinity wedge associated with the SSC extends much farther westward than the core of observed inflow velocities. This may be due to recirculating waters, which originate north of the Faroe Plateau and mix with NAW south of the Norröna's Southern route, after traversing southward along the western edge of the FSC.

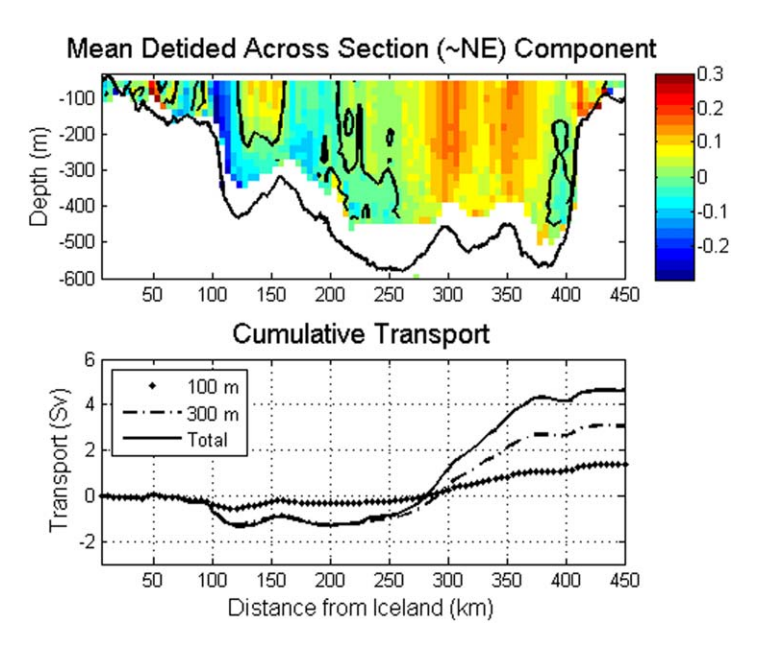


**Figure 8.** Mean ~NE velocities normal to (top) the IFR track and (bottom) cumulative across track transport. The black solid line includes all available data from March 2008 to June 2012 and includes 54 transect crossings.

# 3.2. Flow Across the Iceland Faroes Ridge

Largely, depth-independent inflows appear over the southeastern half of the IFR section with outflows confined to the Iceland side (Figures 7 and 8). Outflow transports are bottom intensified, with almost no measurable outflowing volume flux within the upper 100 m of the western IFR. To the east, inflow transport gradually increases with integration depth. Sampling over the IFR is least reliable on the western side of the section (eastern slope of Iceland), but most of the top 300 m has been observed on more than 25 separate occasions. Means over the IFR are the composite of 54 individual transect crossings and resulting standard errors range

from 0.7 to 5.8 cm/s per bin. Highest error values exist on the Icelandic shelf, where observations are limited, and the Faroese shelf where the velocities are more variable. The resultant integrated transport error over all the full depth range of the IFR section is 0.5 Sv.

High short-term variability and eddy activity over the ridge region introduce fluctuations over a large range of timescales, thus the similarity in the average annual northeast velocity profiles for the years 2010 through 2012 is striking (supporting information Figure S6). Annual means are heavily weighted toward the summer months when data collection is most successful, introducing additional uncertainty to the annual averages. However, little seasonal variation in transport has been observed over the IFR by others [Hansen et al., 2008], despite the observation of increased crossings of the IFR by drifters in the summer by Valdimarsson and Malmberg [1999].

Annual averages from years 2010 to 2012 comprise at least 10 transect crossings each and have strong similarities in structure. Namely, a strong inflow appears over the eastern half of the channel and other than a narrow band of inflow from 100 to 150 km east of Iceland, limited northeasterly flow exists over the western half of the channel. The lateral position of the zero velocity contour in the central channel and the depth of the inflow to the Nordic Seas on the Iceland side vary interannually (supporting information Figure S6). Since the magnitude of the inflow shows little temporal variation, the average annual width of the inflow is logically related to the northeast transport for that year. Annual averages over the IFR section indicate that wider inflows, such as in 2010 and 2012, carry on the order of 9 Sv of Atlantic Water over the ridge, while in 2011, when the inflow narrows to  $\sim$ 150 km, the volume flux drops to around 5 Sv. The average flow over the IFR from March 2008 to June 2012, incorporating the outflows on the Icelandic side, is 4.6  $\pm$  0.5 Sv, split into 5.9 Sv of inflow and 1.3 Sv of outflow (Table 1).

### 4. Discussion

Both the FSC and IFR are subject to fluctuations over a wide range of timescales, and understanding the locations and magnitude of the variations in velocity and hydrographic properties is a critical step in moni-

<b>Table 1.</b> Average Surface Transport Across Each Section in Sv			
	Total	North (East)	South (West)
FSC Middle FSC Southern IFR	1.7 ± 0.2 1.1 ± 0.2 4.6 ± 0.5	3.4 4.0 5.9	-1.7 -2.9 -1.3

toring the AW flux into the Nordic Seas. Short-term processes can significantly alter the position of inflows, as evidenced by the ADCP velocities and more recently by XBT deployments taken monthly across each section (Figure 9). These profiles show that even the strong Shetland Slope Current and inflows over the western Faroese slope change both

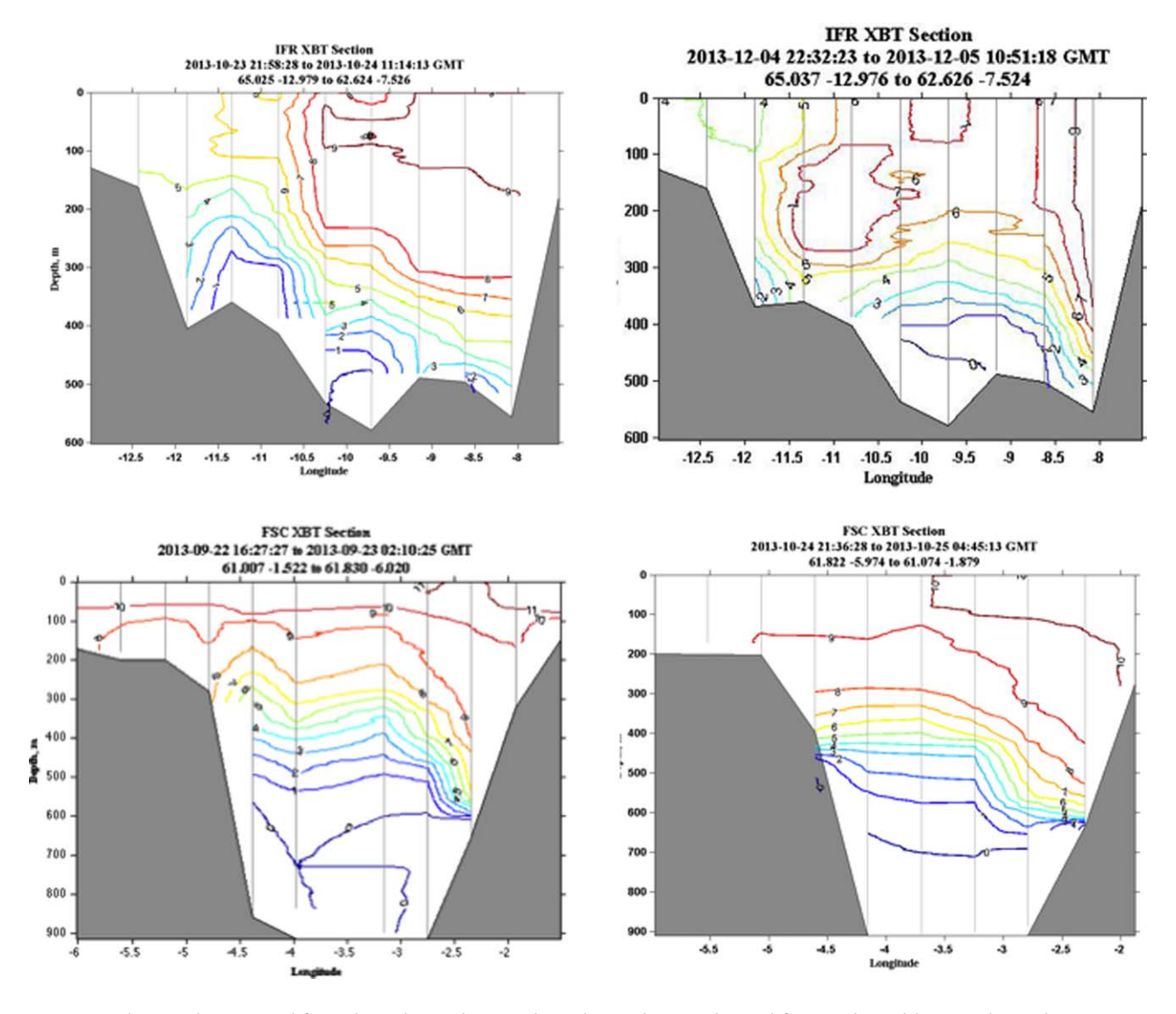
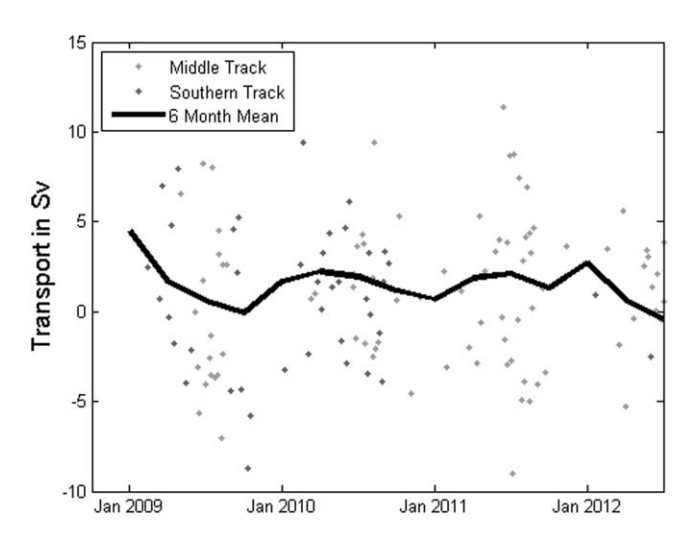


Figure 9. XBT sections taken over the IFR in (top left) October and (top right) November and across the FSC in (bottom left) September and (bottom right) October. Temperature contours are in degrees Celsius and inconsistencies in the topography are due to slight variations in the ship's track with each crossing.

position and depth over a 1 month period. However, constraining this movement and visibly adjusting the flow (for instance the location of the cold overflow in the IFR sections) is the strong influence of topography. We consider here the temporal and spatial characteristics of the FSC and IFR separately, as well as their relation to previous observations of the ridge system.

## 4.1. Temporal and Spatial Characteristics of the FSC

Temporal variations in the week-to-week sections are large, but 3–6 month averages quickly recover the familiar mean structure of the FSC circulation. This is illustrated in Figure 10, which is a composite of the transports from each section crossing of either FSC transect with greater than 80% spatial coverage over the upper 200 m (gray dots) and a 6 month running mean of all sections. Rather than using all the available data for each geographical bin, as in the average section transport calculation, this time series reflects the mean transport over each weekly transect crossing by the Norröna with spatial gaps filled through linear interpolation of the across section velocities to their nearest available neighbors. The time series clearly illustrates the large short-term fluctuations in transport through the channel, but the 6 month mean shows some indication of the overall variation in transport strength form the first 2 years of observation to the latter 1.5 years. Transport structure and magnitude through the FSC are similar to previously reported values and are augmented by coverage of the Faroese shelf shallower than the 300 m isobath, often excluded



**Figure 10.** Time series of FSC section averages (gray dots) and 6 month running mean. Spatial gaps in the cross-transect velocities for each week of more than 80% data coverage were filled using a linear interpolation to nearest neighbors. The standard error from the mean for all available FSC sections (including both the Middle and Southern routes) is 0.4 Sv.

from prior estimates. Using the location of the westernmost moored ADCP along the FIM line as the starting point for cross-channel transport integration, as in most previous studies [Sherwin et al., 2008; Hughes et al., 2006], we find a net transport of 2.2  $\pm$  0.2 Sv toward the Nordic Seas, comparable to the 2.7 Sv observed by Berx et al. [2013] and lower than the 3.5 Sv and 3.9 Sv reported by Sherwin et al. [2008] and Hughes et al. [2006], respectively. Since each estimate incorporates many years of ADCP, hydrographic, and in the case of Berx et al. [2013] altimetric, observations we expect that time variability is not the source of the discrepancy. Instead it may be attributable to fine scale structure over the central

channel that can be resolved more accurately with the vessel mounted ADCP, or related to the varying definitions used to determine the bottom boundary of Atlantic Water depth, which were defined using a 3-point mixing model [Hughes et al., 2006] and 500 m depth [Sherwin et al., 2008]. Older estimates by Tait [1957] and Dooley and Meincke [1981] which relied on geostrophic calculation over an upper layer, defined as above 550 m and with salinity less than 35 PSU, are 2.3 Sv and 2.0 Sv, respectively, closer to the average transports across the Norröna sections. A lack of winter data (supporting information Figure S1) prevents an accurate estimation of the annual cycle, however, based on three seasons of observations we find a seasonal cycle of 0.8 Sv with a maximum in February. This is not inconsistent with recent findings by Berx et al. [2013] of seasonal fluctuations of 0.7 Sv with a winter maximum.

Using the 300 m isobath as the western integration boundary, most previous literature for this region failed to capture the persistent, depth-independent southward flow on the Faroese shelf and upper slope. This flow crosses over the Middle track between approximately 125 and 245 km from the Faroes and over the Southern track from 125 to 175 km from the Faroes with a magnitude ranging from -0.4 to -1.9 Sv annually. Temporal variations in the outflow transport exist, with the current appearing in 67% of Middle track transect crossings and 74% of Southern transect measurements. Of the remaining periods of data collection, a widening of northeastward flows in the central channel partially or fully mask the outflow. Hydrographic factors may be largely ruled out as the source of discrepancy between the two FSC tracks, since the  $\sigma_t = 27.8$  isoline remains at a similar depth between the FSC transects, and large stationary eddies such as those described by *Chafik* [2012] are too large to account for changes over such a short distance. This leaves temporal variations in this southerly flow over the Faroese shelf as the most likely cause of the difference in transport through the FSC sections. The magnitude of interannual transport variations in the southward outflow is larger than those in the Shetland Slope Current and may significantly affect observations of total transport across the Iceland Faroes Shetland ridge.

Present throughout this analysis are the implications of topography and the steering of flows by the bathymetry. This is evident in the strong tendency of the Shetland Slope Current to hug the eastern slope of the FSC over the region of steepest topography and the increased variability over the deeper and more stratified central channel. This can be quantitatively expressed by correlating a time series of velocities to nearby f/H contours. The tight relationship between topography and the largely depth-independent flows over the shelves and slopes of both sections is not surprising. Following this line of reasoning, and noting the similarity in tidal excursion and characteristic current length scale, tidal rectification is expected [Zimmerman, 1978, 1981; Robinson, 1981] and in fact has been observed by Larsen et al. [2008] following the shelf bathymetry around the Faroes in water shallower than 200 m. It is possible that the strong southward flow we observe farther east of the Faroes, along the outer edges of the shelf, may also be influenced by the tides, but it is more likely that the

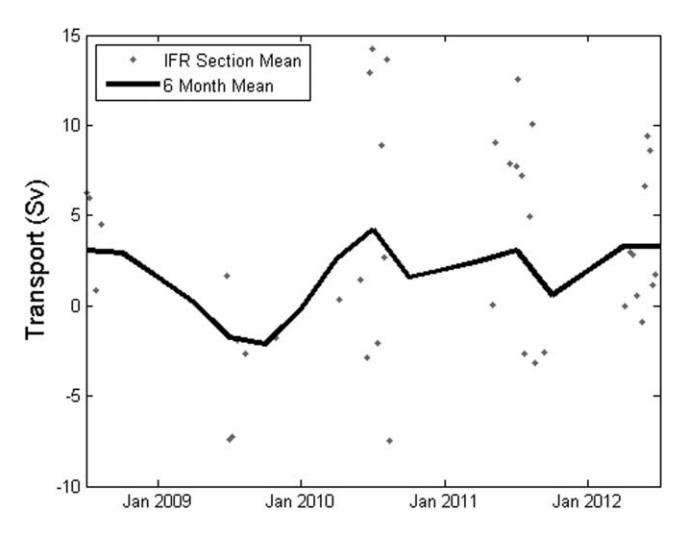


**Figure 11.** Time series of IFR section averages (gray dots) and 6 month running mean. Spatial gaps in the cross-transect velocities for each week of more than 80% data coverage were filled using a linear interpolation to nearest neighbors. The standard error from the mean for all available IFR sections is 0.8 Sv.

deeper flows along the Faroese slope are related to inflows over the IFR. These waters may have circulated east then south into the FSC before bending northward and joining the Shetland Slope Current. The precise behavior and magnitude of recirculating flow should become more evident with increased coverage by the XBT program and the ability to separate recent Atlantic Water inflows from those exposed to mixing with water from the Nordic Seas.

# 4.2. Temporal and Spatial Characteristics of the IFR

Similar to the FSC, the weekly and monthly variations in IFR section transport are large (Figure 11), but despite large short-term fluctuations,

the consistency of spatial characteristics becomes particularly evident as coverage improves. This is especially true for the latter years of observation (2010–2012) when there was an increase in IFR data coverage, both spatially and temporally. The lateral width of the inflowing velocities over the eastern half of the section vary by up to 50 km and may be associated with the strength of the inflow or the angle of crossing, with the inflow expanding westward during years when the magnitude of the northeast velocity is greatest. The presence of a small, surface intensified inflow between 100 and 150 km east of Iceland, Figure 8, is indicative of the influence of flows along the IFF. This sharp temperature and density front tend to meander along the northern slope of the IFR.

The observed large fluxes of Atlantic Water across the IFR are worth noting here. These estimates may even be under-representative of the full inflow. Summing the average transport through the bottom-most bin and extending these values to the seafloor over the eastern (inflowing) half of the section increases the mean flow across the IFR by 0.9 Sv. The inclusion of surface outflows on the western edge of this section into the average surface transport may also cause the average IFR inflow to be an underestimate of the total AW flux, since western outflows not be AW, but instead related to the East Icelandic Current [Malmberg and Kristmannsson, 1992]. The observed 5.9 Sv mean inflow value appears high compared to the 3.5  $\pm$  0.5 Sv reported by Hansen et al. [2003, 2010], using line N observations of temperature, salinity, and moored velocity profiles along a section extending directly north of the Faroes. Those papers defined the mean depth of the 35.05 isohaline as the southern-most boundary for inflowing AW. Historical hydrographic data available from ICES over a similar temporal and spatial section show salinity values close to or slightly below 35 PSU over the deeper and western edges of the observed IFR inflow. We consider here that as the Atlantic Water crosses the IFR, it is prone to mix with cooler and fresher Nordic Sea waters. This mixing may change the hydrographic character of the flow considerably, reducing its salinity to below 35.05 PSU and resulting in an apparent "disappearance" of Atlantic Water between the Norröna's IFR transect and the observations along line N. This is particularly true for the deeper waters at depths greater than 500 m, and during periods when the width of the inflow has extended westward, potentially entraining some of the less saline water on the Icelandic side and resulting in a loss of the characteristic high salinity of NAW. A detailed analysis of the effect of mixing on the hydrography of the IFF and IFR region can be found in Beaird [2013] and is beyond the scope of this analysis, but significant differences in the inflows reported here as compared to those found in Hansen et al. [2003, 2010] may be attributable to differing definitions of the lower bounds of IFR inflows.

### 5. Summary

Repeated observations along standard sections in the IFR and FSC offer an accurate estimate of volume flux into the Nordic Seas. In total, approximately  $6.1\pm0.3$  Sv of directly observed surface transport crosses the

Iceland Faroes Scotland Ridge, with  $4.6\pm0.5$  Sv entering over the full depth of the IFR and  $1.5\pm0.2$  Sv above the  $\sigma_t=27.8$  isopycnal, through the FSC. This shows an overall increase from earlier observations of the FSC by this program due to a weakening of along isobath southward flows on the western slope of the FSC, and emphasizes the importance of long-term observations in this region. A difference in the average transport through the two FSC sections also highlights the temporal variability through the channel. This occurs despite the high spatial consistency of currents within the FSC. Similarly, when averaged over periods long enough to remove short-term eddy processes, flows over the IFR maintain their basic structure over all years of data collection with variations in northeast transport related to the width of inflow.

As expected, the surface flows are tightly coupled to the bathymetry of each section, especially over the steep slopes and shallow shelves. The ability of the topography to influence the relatively fine scale structure of the currents in this region is particularly evident in this method of data collection, which is of higher spatial resolution than satellite or moored current meter observations of the region. The addition of an XBT program earlier this year will improve estimates of heat flux across the ridge and offer a clearer image of the water mass structure and variability.

#### Acknowledgments

The authors thank Jógvan i Dávastovu and Smyril Line for their continued help and support. We thank Sandra Anderson-Fontana for all of her support and for processing the ADCP data. We extend our thanks to Peter Rhines and two anonymous reviewers, whose comments have significantly improved the clarity of this paper. We are grateful to the National Science Foundation for its support of the project through grants 04552274 and 1060752 to Stony Brook University and grants 0452970 and 1061185 to the University of Rhode Island.

## References

Beaird, N. L. (2013), Meridional exchanges and mixing at the Iceland-Faroe Ridge, PhD thesis, University of Washington, Seattle, Wash. Berx, B., B. Hansen, S. Østerhus, K. Larsen, T. Sherwin, and K. Jochumsen (2013), Combining in situ measurements and altimetry to estimate volume, heat and salt transport variability through the Faroe-Shetland Channel, *Ocean Sci.*, 9, 639–654.

Borenäs, K. M., I. L. Lake, and P. A. Lundberg (2001), On the intermediate water masses of the Faroe-Bank Channel overflow, *J. Phys. Ocean-*

Chafik, L. (2012), The response of the circulation in the Faroe-Shetland Channel to the North Atlantic Oscillation, *Tellus, Ser. A, 64,* 18,423. Coachman, L. K., and K. Aagaard (1974), *Physical Oceanography of Arctic and Subarctic Seas*, Springer, Berlin.

Dooley, H. D., and J. Meincke (1981), Circulation and water masses in the Faroese channels during overflow '73, *Dtsch Hydrogr. Z.*, 34(2), 41–55. Dunn, M. (2002), A description of the barotropic tide on Georges Bank based upon five years of shipboard ADCP observations, PhD thesis, State Univ. of New York at Stony Brook, Stony Brook, N.Y.

Egbert, G. D., and S. Y. Erofeeva (2002), Efficient inverse modeling of barotropic ocean tides, *J. Atmos. Oceanic Technol.*, 19(2), 183–204.

Gaard, E., and B. Hansen (2000), Variations in the advection of *Calanus finmarchicus* onto the Faroe Shelf, *ICES J. Mar. Sci.*, 57(6), 1612–1618.

Häkkinen, S., P. B. Rhines, and D. L. Worthen (2013), Northern North Atlantic sea-surface height and ocean heat content variability, *J. Geophys. Res. Oceans*, 118, 3670–3678, doi:10.1002/jgrc.20268.

Hansen, B., S. Østerhus, H. Hátún, R. Kristiansen, and K. M. H. Larsen (2003), The Iceland-Faroe inflow of Atlantic water to the Nordic Seas, *Prog. Oceanogr.*, 59(4), 443–474.

Hansen, B., S. Østerhus, W. Terrell, S. Jonsson, H. Valdimarsson, H. Hatun, and S. Olsen (2008), The inflow of Atlantic Water, heat, and salt to the Nordic Seas across the Greenland-Scotland Ridge, in *Arctic-Subarctic Ocean Fluxes*, pp. 15–43, Springer, Dodrecht, Netherlands.

Hansen, B., H. Hátún, R. Kristiansen, S. Olsen, and S. Østerhus (2010), Stability and forcing of the Iceland-Faroe inflow of water, heat, and salt to the Arctic. Ocean Sci., 6, 1013–1026.

Helland-Hansen, B., and F. Nansen (1909), The Norwegian Sea, Rep. on Norwegian Fish. and Mar. Invest. 2, vol. 390, Kristiania, Norwegian Fisheries and Marine Investigations, Bergen, Norway.

Hughes, S. L., W. R. Turrell, B. Hansen, and S. Østerhus (2006), Fluxes of Atlantic Water (volume, heat and salt) in the Färoe-Shetland Channel calculated from a decade of Acoustic Doppler Current Profiler data (1994–2005), Fish. Res. Serv. Collab. Rep. 01/06, Fisheries Research Services Marine Laboratory, Aberdeen, Scotland.

Jakobsen, P. K., M. H. Ribergaard, D. Quadfasel, T. Schmith, and C. W. Hughes (2003), Near-surface circulation in the northern North Atlantic as inferred from Lagrangian drifters: Variability from the mesoscale to interannual, *J. Geophys. Res.*, 108(C8), 3251, doi:10.1029/2002JC001554. Larsen, K. M. H., B. Hansen, R. Kristiansen, and S. Østerhus (2000), Internal tides in the waters surrounding the Faroe Plateau, in *Proceedings* 

of ICES 2000 Annual Conference, ICES Annual Science Conference, Bruges, Belgium. Larsen, K. M. H., B. Hansen, and H. Svendsen (2008), Faroe shelf water, Cont. Shelf Res., 28(14), 1754–1768.

Malmberg, S. A., and S. Kristmannsson (1992), Hydrographic conditions in Icelandic waters, 1980–1989, ICES Mar. Sci. Symp., 195, 76–92. Robinson, I. (1981), Tidal vorticity and residual circulation, Deep Sea Res., Part A, 28(3), 195–212.

Rossby, T., and C. Flagg (2012), Direct measurement of volume flux in the Faroe-Shetland Channel and over the Iceland-Faroe Ridge, *Geophys. Res. Lett.*, 39, L07602, doi:10.1029/2012GL051269.

Sherwin, T., S. Hughes, W. Turrell, B. Hansen, and S. Østerhus (2008), Wind-driven monthly variations in transport and the flow field in the Faroe-Shetland Channel, *Polar Res.*, 27, 7–22.

Tait, J. B. (1957), Hydrography of the Faroe-Shetland Channel, 1927–1952, HM Stn. Off., Edinburgh.

U.S. Department of Commerce, N. O. A. A., and N. G. D. C. Atmospheric Administration (2006), 2-Minute Gridded Global Relief Data (ETOPO2v2). [Available at http://www.ngdc.noaa.gov/mgg/fliers/06mgg01.html.]

Våge, K., R. S. Pickart, M. A. Spall, G. Moore, H. Valdimarsson, D. J. Torres, S. Y. Erofeeva, and J. E. Ø. Nilsen (2013), Revised circulation scheme north of the Denmark Strait, *Deep Sea Res., Part 1, 79,* 20–39.

Valdimarsson, H., and S. A. Malmberg (1999), Near-surface circulation in Icelandic waters derived from satellite tracked drifters, *Rit Fiskideild*,

von Appen, W. J., R. S. Pickart, K. H. Brink, and T. W. Haine (2014), Water column structure and statistics of Denmark Strait Overflow Water cyclones. Deep Sea Res., Part I. 84, 110–126.

Wang, Y. H., L. Y. Chiao, K. M. Lwiza, and D. P. Wang (2004), Analysis of flow at the gate of Taiwan Strait, J. Geophys. Res., 109, C02025, doi: 10.1029/2003JC001937.

Zimmerman, J. (1978), Topographic generation of residual circulation by oscillatory (tidal) currents, *Geophys. Astrophys. Fluid Dyn.*, 11(1), 35–47. Zimmerman, J. (1981), Dynamics, diffusion and geomorphological significance of tidal residual eddies, *Nature*, 290, 549–555, doi:10.1038/290549a0